INFLUENCE OF IMPERFECTIONS ON AXIAL BUCKLING LOAD OF COMPOSITE CYLINDRICAL SHELLS

J. Kepple[1,2*], B. G. Prusty[1], G. Pearce[1], D. Kelly[1], R. Thomson[2,3], R. Degenhardt[4]
[1] School of Mechanical and Manufacturing Engineering, The University of New South Wales, Sydney, Australia, [2] Cooperative Research Centre for Advanced Composite Structures, Melbourne, Australia, [3] Advanced Composite Structures Australia Pty Ltd, Melbourne, Australia, [4] Institute of Composite Structures and Adaptive Systems, German Aerospace Centre (DLR), Braunschweig, Germany.
* Corresponding author (jendi.kepple@unsw.edu.au)

Keywords: *buckling, monocoque cylinder, robust optimization, spectral representation*

1 Introduction

There is a strong requirement for more robust, lighter and cheaper launch vehicle structures. Unstiffened composite cylindrical shells, which are essential to the fabrication of launch vehicle airframes, are prone to buckling and are highly sensitive to imperfections which arise during the manufacturing process. The buckling load is an important characteristic in design, and may vary drastically from the buckling load of the perfect structure when realistic imperfections are present. [1]

The current design guidelines for imperfection sensitive shells are based on the NASA-SP 8007 [2] which dates from 1965. Typically, the theoretical buckling load of a given cylinder design is predicted by performing a linear bifurcation analysis using closed-form equations of the geometrically perfect structure. This theoretical buckling load is then reduced by applying an empirical knockdown factor to account for the differences between theory and test.

From recent literature [3-5], the NASA-SP 8007 knockdown factors used in the design of aerospace-quality shell structures were found to be overly conservative and inappropriate for shells constructed from modern manufacturing processes and materials such as composites. Such a conservative approach means that structures are therefore heavier and more costly than need be.

Dependable and verified design criteria for thin-walled cylindrical shells are required, particularly for shells constructed from advanced materials and manufacturing techniques. A new design criterion using a new robust optimization methodology in conjunction with the Single Perturbation Load Approach (SPLA) and the stochastic approach is being developed by the collaborative European 7th Framework Program project: New Robust Design Guideline for Imperfection Sensitive Composite Launcher Structures (DESICOS) [6]. The design criterion will account for real behavior of composite materials including imperfections to provide less conservative and more accurate knockdown factors.

This paper provides a measure of the *Sensitivity* and *Influence* of initial imperfections on the axial buckling load of 50 nominally identical composite cylinders which were numerically generated from actual shell measurements [5], as a contribution to the overall DESICOS project. The effect of initial geometric, loading, thickness and material imperfections on the axial buckling load of unstiffened composite cylindrical shells was investigated and compared using probabilistic finite element (FE) analysis in conjunction with the stochastic approach and metamodels. The magnitudes of the imperfections were plotted against the axial buckling load and the effect of each imperfection type on the overall axial buckling load determined. The results displayed may be used for the robust optimization of shells which may improve the reliability of their knock-down factors.

2 Influence of Imperfections

Preliminary investigations into the influence of loading and geometrical imperfections were conducted by Zimmermann [7] and further developed by Hühne et al. [8]. It was discovered that the effect of the imperfections depend on laminate set-up. The results from Hühne et al. [8] can be used

to define lower limits for knock-down factors of composite shells and provide a direction for the design engineer regarding which manufacturing tolerances to focus on. The results also indicate that the downside of achieving higher buckling loads is that the designs are more sensitive to geometrical imperfections.

Hühne et al. [8] quantified the imperfection loading energy in terms of the area underneath the peak load experienced at the circumference of the cylinder. The influence of loading imperfections was then compared to that of geometrical imperfections.

More recently, Degenhardt et al. [5] investigated the imperfection sensitivity of geometrical and non-traditional imperfections such as loading, material and thickness imperfections using probabilistic methods. The work presented here re-evaluates and extends that of Hühne et al. [8] and Degenhardt et al. [5] to compare and evaluate imperfection sensitivities through a proposed technique to non-dimensionalise the responses as a means of dealing the different fundamental units. Lastly, the sensitivity of the axial buckling load to imperfections is rigorously investigated by adopting and enhancing the stochastic methods developed by Lee et al. [9].

3 Stochastic Modeling of Imperfection Types

Full scale initial measurements of thickness and geometric imperfections of eight nominally identical CFRP IM6/8557 UD cylinders from a DLR paper (Degenhardt et al. [5]) were imported into MSC.Patran/Nastran for SOL 106 non-linear static analysis. These cylinders are representative of imperfection sensitive design in which the sensitivity of the axial buckling load to each imperfection type is magnified. An overview of the nominal cylinder data is provided in Table 1.

Table 1. Nominal properties of DLR cylinders.

Property	Nominal Data
Total length (mm)	540
Free length (mm)	500
Radius (mm)	250
Total Thickness (mm)	0.5
Lay up	[24/-24/41/-41]
Cylinder mass (g)	641

In the lay-up presented in Table 1, the 24º ply is the innermost ply and all plies have the same thickness of 0.125mm.

For convergence studies different mesh refinements (between 1,500 and 80,000 elements) were used from which a benchmarked model of 14,400 elements was selected. In addition, different boundary conditions were tested resulting in a benchmarked clamped bottom edge (in all three translational degrees of freedom) and a displacement controlled upper edge as shown in Figure 3. The boundary conditions were applied to 20mm axial length on the top and bottom edges to simulate the epoxy resin potting from [5].

The Z26 cylinder from Degenhardt et al. [5] was simulated as the “perfect” benchmark model. Actual measured initial geometric and thickness imperfections were then added onto the perfect cylinder simulation and compared with test results as shown in Figure 1. Although variations in thickness reduce the overall buckling load, geometric imperfections reduce the load more significantly. When both imperfection types are incorporated into the simulation, the combined effect further reduces the global buckling load to a point just above the test value. The difference between the simulation with geometric and thickness imperfections and the test value may be caused by loading imperfections which were not measured in [5]. Deterministic values cannot be assigned to those imperfections and a large number of stochastic simulations are needed to address the influence of the loading imperfection on the axial buckling load of monocoque cylinders.

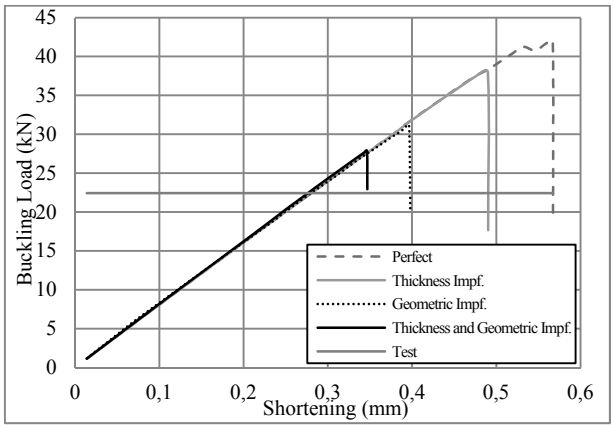

Fig. 1. Comparison of Z26 cylinder load shortening curves from simulations and test results with thickness and geometric imperfections.

3.1 Geometric Imperfections

To accurately model realistic geometric imperfections, ATOS-scanned geometrically imperfect shells [5, 8] were imported into MATLAB, treated as random fields and their evolutionary power spectrum determined. The evolutionary power spectrum was then used in conjunction with the spectral representation method to generate 50 Monte-Carlo computational models of random imperfect 2D shell surfaces [10, 11]. Under the constraints of the evolutionary power spectrum, these surfaces fit within the statistical margins of the initial tested shells. The power spectrum is described as the Fourier transform of the auto-correlation function $R(x,\tau)$ and may be interpreted as the distribution of the mean square of the random field $f(x)$ over the space-frequency domain [11]. The evolutionary power spectrum was decomposed into two unrelated functions for the frequency content and the spatial evolution based on the surfaces' eligibility to utilize the method of separation. This method allows an accurate estimation of the evolutionary power spectrum with a reduced data set and is given as [11]:

$$S(\omega,x) = \tilde{S}(\omega)\tilde{g}(x) \tag{1}$$

where the estimated homogenous Fourier spectrum is:

$$\tilde{S}(\omega) = E\left[\frac{1}{2\pi L}\left|\int_0^L Y_i(x_i)\omega(x-x_i)e^{-I\omega x}dx\right|^2\right] \tag{2}$$

and the estimated spatial envelope is:

$$\tilde{g}(x) = \frac{E[|Y_i(x)|^2]}{2\int_0^\infty \tilde{S}(\omega)d\omega}. \tag{3}$$

The Hamming window was used to reduce the window-processing loss energy bias. For a bi-dimensional random field, the spectral representation method is [11]:

$$Y(x_1,x_2) = \sqrt{2}\sum_{i=0}^{N_1-1}\sum_{j=0}^{N_2-1}\left[A_{ij}cos(\omega_{1i}x_1+\omega_{2j}x_2+\phi_1) + A_{ij}cos(\omega_{1i}x_1-\omega_{2j}x_2+\phi_2)\right] \tag{4}$$

where

$$A_{ij} = \sqrt{2S(\omega_{1i},\omega_{2j},x_1,x_2)\Delta\omega_1\Delta\omega_2}. \tag{5}$$

All variables have their common meanings [10, 11]. An example of an imperfect surface generated using this approach is shown in Figure 2.

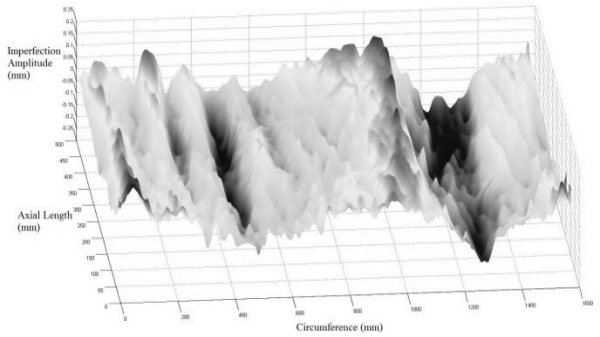

Fig 2. Bi-dimenional random field generated using the spectral representation method.

The spectral representation method generates new imperfect surfaces based about a common mean or average value. Having passed the Kolmogorov-Smirnov test (KS-test), which was used to check whether the distribution of any small statistical series can be approximated by a normal distribution [12], measured average radii of the cylinders, among other variables, were confirmed to conform to a Gaussian normal distribution with the parameters shown in Table 2.

Table 2. Gaussian parameters of CFRP cylinders.

Parameter	Mean (mm)	Standard Dev. %
Radius	250.743	0.014
Total Thickness	0.478	2.699

The values in Table 2 were then used to generate 50 different mean radii and thickness values which were incorporated into the 50 FE simulations.

3.2 Thickness Imperfections

Automated ultrasonic tests on the actual cylinders were conducted by DLR using the water split coupling echo-technique to detect any defects in the structure; such as delaminations or air pockets [5]. Thickness imperfections were also recorded using this technique and imported into the spectral representation method to create 50 stochastic models with various correlated thickness measurements; an example of which is shown in Figure 3.

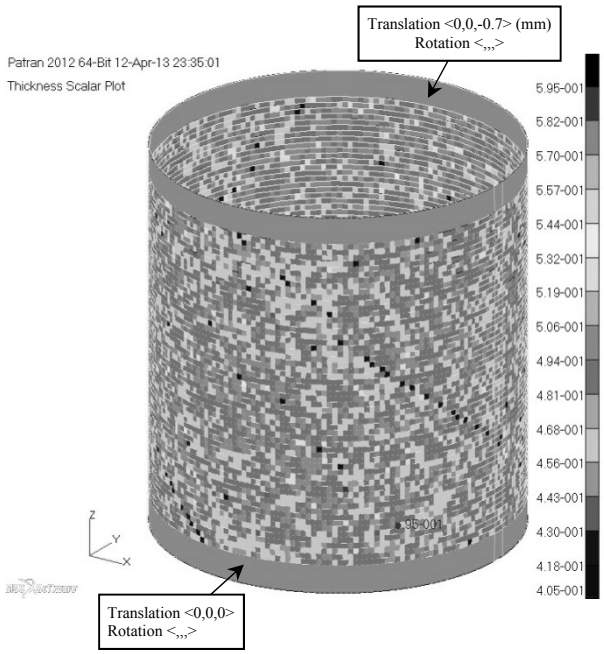

Fig. 3. FE model featuring boundary conditions and thickness imperfections generated from the spectral representation method.

In addition to the spectral representation method, the means of the thickness imperfections for each cylinder were varied according to the Gaussian distribution in Table 2.

3.3 Material Imperfections

Material imperfections are often characterized from literature or provided from the manufacturer in terms of their tested mean and standard deviation values. The probabilistic material properties of the cylinders were given in [5] following several different studies. From benchmarked results, the values chosen for the stochastic FE models are displayed in Table 3.

Table 3. Material Properties of measured CFRP prepreg IM7/8552 UD, Gaussian normal distributed means and standard deviations [5] t = tension, c = compression, L = longitudinal direction, and T = transverse direction

Stiffness Properties	Mean value (GPa)	Standard Deviation (%)
E_{cL}	157.4	2.39
E_{cT}	10.1	4.11
G_{LT}	5.3	1.10
Poissońs Ratio	0.31	5.55

The material properties displayed in Table 3 were incorporated into MATLAB to generate 50 different material properties for the stochastic simulations.

Variations in material properties are often much higher in composite shells than those manufactured from isotropic materials. Such variations are unavoidable using modern manufacturing techniques and arise from the intrinsic anisotropy of composite materials [13]. From the DLR ultrasonic scans and Figure 3, it is evident that some points with the lowest thicknesses are situated along the fibre directions; particularly the outermost -41° ply. These aligned points can be interpreted as a gap between plies in that particular direction which was not adequately closed during fabrication [10]. These areas therefore possess different localized material properties.

An automated routine [10] was followed in order to pinpoint aligned areas where inter-ply gaps may exist. Firstly, all points that were characterized as the absolute lowest thickness value were selected as candidate gap points. If the points were aligned in ply directions and exceeded a certain threshold, set at one-fifth the total number of points in the ply direction, a missing ply was assigned to these points. Otherwise, they were modeled by a reduction in the matrix phase only.

3.3 Loading Imperfections

Hühne et al. [8] employed the compression test facility shown in Figure 4 and utilized shims to induce unevenness in the end plates for realistic loading imperfections.

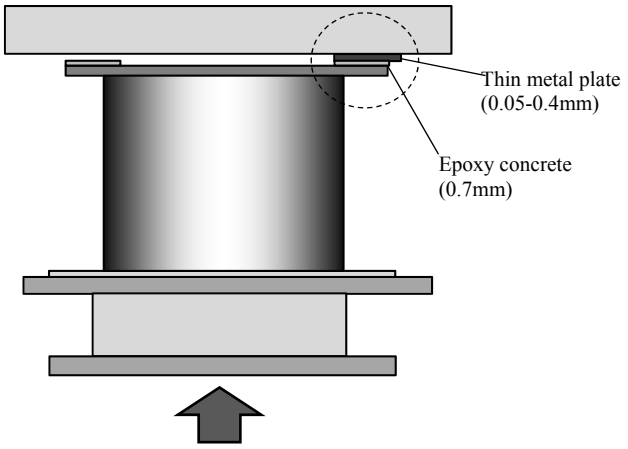

Fig. 4. Load introduction with shim to induce an uneven loading over the entire upper edge [8].

The shim used was a thin metal plate with a thickness that varied from t = 0.05mm to t = 0.4mm. It was located between the top and the end plate at 32 predefined and equally spaced positions on the circumference and provided the stochastic input into these simulations.

To represent the above loading imperfections in MSC.Patran, an uneven "initial displacement" was applied over the upper edge of the cylinders, where the maximum initial displacement corresponded to the various thicknesses of the metal shim; an example of which is shown in Figure 5.

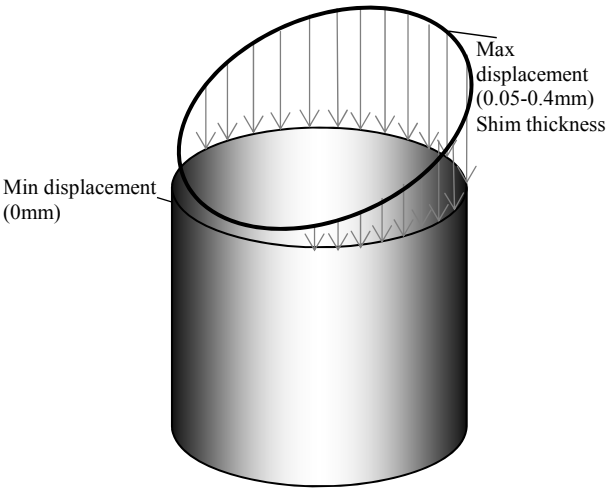

Fig. 5. Load imperfection simulation in MSC.Patran.

The largest magnitudes of the simulated loading imperfections were placed randomly around the circumference for additional stochastic variation. The upper circumferential edge was then displaced downwards by the boundary conditions shown in Figure 3 which represent the compression force induced by the buckling tests.

4 Effect of Various Imperfection Types on Axial Buckling Load

Two formulations, the *Influence* and *Sensitivity*, can be used to provide insight on the effect that each imperfection type (or input variable) has on the axial buckling load (or output variable) from metamodels [9].

4.1 Derivation of Sensitivity

Sensitivity can be determined by using the least-squares method (Legrende [14]). This is a measure of the gradient of the output results with respect to an input variable. The axial buckling load (output) and the difference between the magnitude of the different imperfection types (input) and their average values were plotted into metamodels and their sensitivities defined using the following formula [9]:

$$\beta = \frac{\sum_{i=1}^{m}(X_i - \bar{X})(Y_i - \bar{Y})}{\sum_{i=1}^{m}(X_i - \bar{X})^2} \tag{6}$$

where β is the "sensitivity" of the output with respect to a given input,
m is the number of stochastic inputs,
Y_i is the output response,
X_i is the input variable; and,
the over-bar indicates the mean value.

The values of the sensitivities were scaled and normalized ($N\beta$) to remove skew effects originating from the different fundamental units of the stochastic inputs [15]. The sensitivity points to the amount of change that the output result experiences with respect to a change in the input variable. Thus, a large *Sensitivity* translates to a large change in output, as the input is varied. This is shown in Figure 6 where plots showing various levels of sensitivity are shown. Note that *Sensitivity* can also be interpreted as the gradient of the line of best fit for any given metamodel.

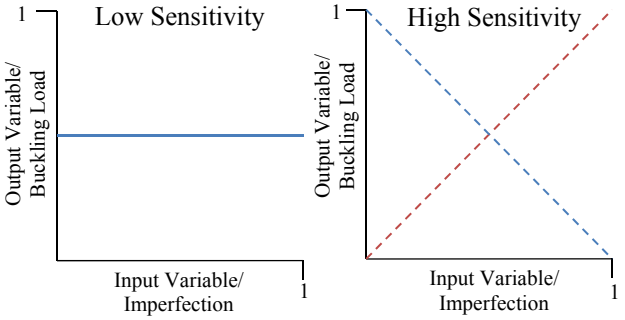

Fig. 6. Sensitivity is the gradient of the best-fit line between the input and output.

4.2 Derivation of Influence

A measure of the correlation of the output result with respect to the input variable is also necessary to determine the overall effect of various imperfections on the axial buckling load. This correlation is a measure of the *Influence* that the input variable has over the behavior of the response. The Spearman Correlation [16] was selected as it is neither biased nor is there a requirement for the variables to be

linearly related. The formulation for the *Influence* ρ is:

$$\rho = \frac{\sum_{i=1}^{m} R(X_i)R(Y_i) - m\left(\frac{m+1}{2}\right)^2}{\sqrt{\sum_{i=1}^{m} R(X_i)^2 - m\left(\frac{m+1}{2}\right)^2}\sqrt{\sum_{i=1}^{m} R(Y_i)^2 - m\left(\frac{m+1}{2}\right)^2}} \quad (7)$$

where R is the ordinal rank,
Y_i is the output response,
X_i is the input variable; and,
m is the number of samples in the metamodel.

An *Influence* factor of unity means that the input is directly proportional to the output. Alternatively, an *Influence* factor of -1 means that the input variable is inversely proportional to the output. An *Influence* factor of 0 means the input variable has no influence on the behavior of the output response as described in Figure 7.

Fig. 7. Influence represents the correlation of the input to output.

4.3 Formulation for Overall Effect

Lee [9] used the *Sensitivity* and *Influence* to formulate an indicator for robustness. Similarly in this case, the *Sensitivity* and *Influence* was used to formulate an index for the overall effect of each imperfection type on the axial buckling load. The indictor was compiled as follows:

$$E_{input} = |N\beta \times \rho| \quad (8)$$

Where E_{input} is an indicator of the overall effect of the imperfection type on the axial buckling load. From the derivations, it is evident that higher magnitudes of *Sensitivity* and *Influence* lead to higher overall effect of the imperfection on the axial buckling load.

The parameters described here can be used in the future to define limits on manufacturing tolerances for robust design.

5 Results

Nonlinear static finite element simulations were performed in which 50 time steps were selected and 10 iterations allowed to convergence. An example of the buckling behavior of an imperfect cylinder is shown in Figure 8.

8a. 8b.

Fig. 8. Buckling behavior of an imperfect cylinder. Just before the onset of global buckling, deep grooves are typically seen near the maximum initial load displacement (shim placement) as shown by the dark colored patch in 8a. Shortly after, global buckling typically commences at a location near the initial local buckle at the mid-length of the cylinder (8b).

Metamodels featuring the results from 50 stochastic FE simulations with various imperfections were determined from the simulations are plotted in Figures 9-15. The values of their *Sensitivity*, *Influence* and overall effect on the axial buckling load are shown in Table 4.

Table 4. Results from stochastic analysis.

	Average Value	$N\beta$	ρ	E_{input}
Geometric	250.743 mm	0.961	0.194	0.186
Total Thickness	0.478 mm	0.991	0.480	0.476
Loading	0.2 mm	-0.940	-0.442	0.416
E_{cL}	157.4 GPa	-0.999	-0.048	0.049
E_{cT}	10.1 GPa	-0.999	-0.238	0.238
G_{LT}	5.3 GPa	-0.999	-0.036	0.036
Poissońs Ratio	0.31	-0.939	-0.097	0.091

The magnitude of the compression and shear moduli were scaled to fit within a 0-0.5 value range to elicit the highest and most conservative normalized sensitivity and to enable comparison with input variables of lower values.

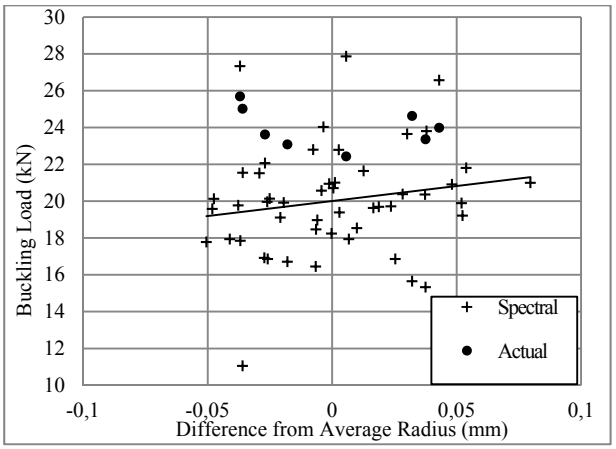

Fig. 9. Effect of geometric imperfections on axial buckling load.

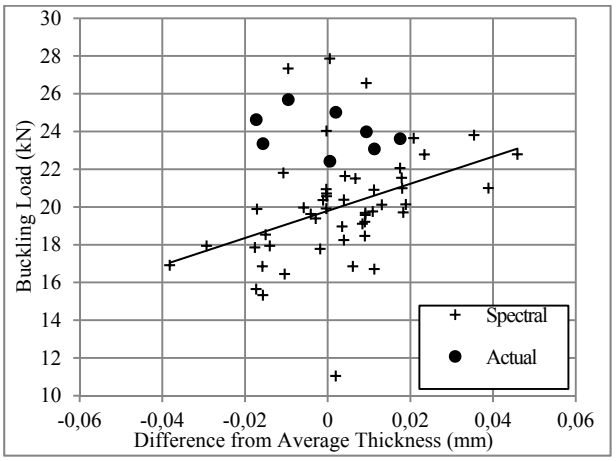

Fig. 10. Effect of thickness imperfections on axial buckling load.

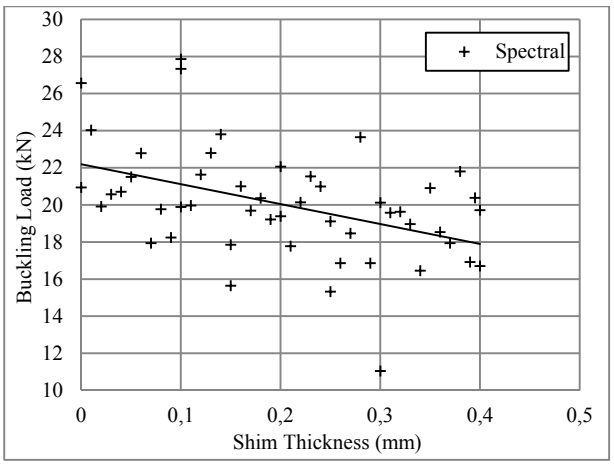

Fig. 11. Effect of loading imperfections on axial buckling load.

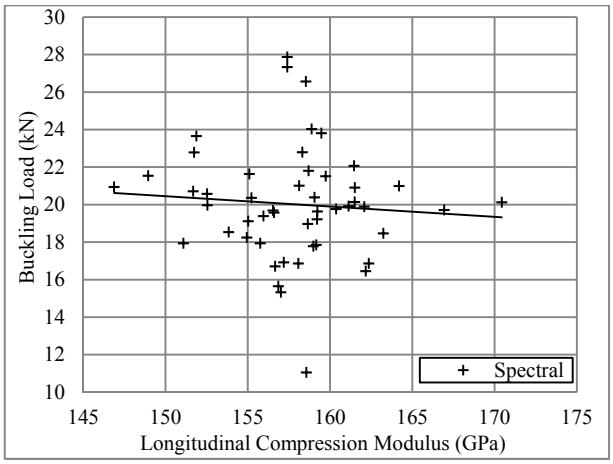

Fig. 12. Effect of longitudinal compression modulus imperfections on axial buckling load.

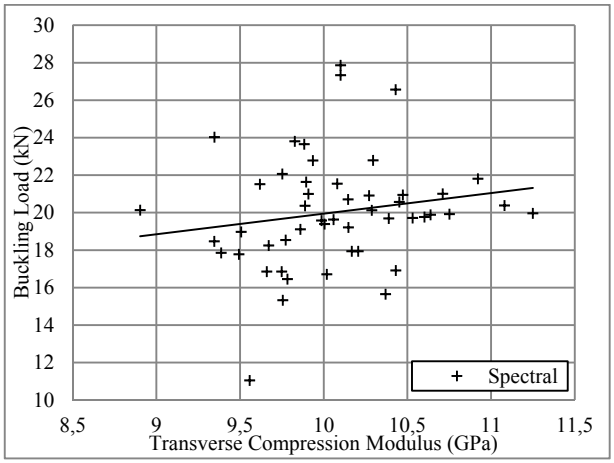

Fig. 13. Effect of transverse compression modulus imperfections on axial buckling load.

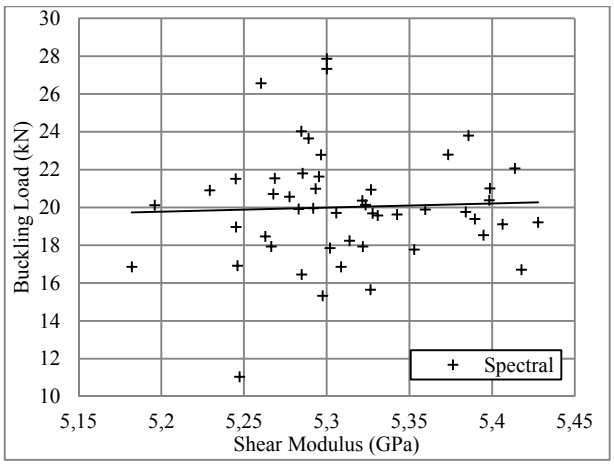

Fig. 14. Effect of shear modulus imperfections on axial buckling load.

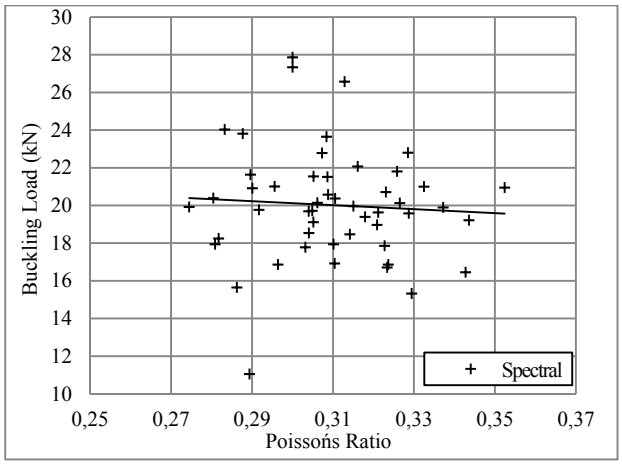

Fig. 15. Effect of Poissońs ratio imperfections on axial buckling load.

6 Discussion

The metamodels agree with intuitive understanding of the variability in the overall buckling load with respect to changes in the cylinder geometry, material and boundary conditions. For instance, it is well understood that as the average radius of the cylinder increases, the overall buckling load should increase, as is the case with upward trend line in the metamodel in Figure 9. Likewise, as the average thickness increases, the general buckling load increases and as the loading imperfection or shim thickness increases, the buckling loads decreases. The same can be said of general material variability except the longitudinal compression modulus, which seems to have little effect on the global buckling load.

Based on the values of E_{input} in Table 4, there is a strong indication that imperfections in the overall thickness play the largest role in determining the overall axial buckling load of imperfection sensitive unstiffened cylinders, followed closely by loading imperfections. For these imperfection types, the axial buckling load is highly correlated to any slight change in its average value. Hardly affecting the axial buckling load are general material imperfections such as the longitudinal compression modulus, the shear modulus and the Poissońs ratio. These findings agree with results from literature [5, 17]. By investigating the correlation of the axial buckling load to various imperfection types through probabilistic analyses, Degenhardt et al. [5] found that geometrical, loading and boundary conditions had the largest overall influence. Thickness imperfections, the longitudinal Young's modulus and deviated fibre angles caused a further load reduction. From investigations on cylinders of similar length and radius, but different lay-ups, Hilburger and Starnes [17] suggest that variations in the thickness can have a significant effect on the buckling load of the shell. Literature [7, 8, 17] also suggests that variations in the laminate set-up, such as ply thickness, stacking sequence and ply angle variation play a large role in determining the overall buckling load of the shell.

Surprisingly, from the results of this stochastic analysis, geometric imperfections rank fourth in its overall effect on the axial buckling load. This particular imperfection type, from literature [18-20], was initially suggested to be the main cause of the large knockdown factors needed to design robust cylinders.

Also unexpectedly, the transverse compression modulus ranks third in its overall effect on the axial buckling load. From previous literature [5], it was suggested that material imperfections, such as the Young's modulus perpendicular to the fibre direction and the shear modulus, play a negligible role in its effect on the axial buckling load.

7 Future Work

The results of this approach to quantifying the sensitivity of various imperfection types on the overall axial buckling load are far from conclusive. Many more stochastic simulations are needed to confirm the validity of this approach for robust design. Monocoque composite cylinders of various lengths, radii, thicknesses and lay-ups are required to validate this approach for unstiffened shells. It is important to determine if thickness imperfections are the governing imperfection type across a range of shell geometries or if these results only apply to the particular shell tested in this paper. This will enable manufacturers to tighten tolerances on the thickness while loosening tolerances on other fabrication parameters to save cost whilst obtaining an optimized robust cylinder design.

Furthermore, stochastic results from stiffened, isogrid and sandwich shells of different material and shapes (conical structures) and physical buckling tests on all structural samples are required to ensure

the validity of this approach across a range of different important structural designs. The correlation of the imperfections to the torsional buckling load may also emerge as an important research topic

Furthermore, variations in fibre angle were not accounted for in this paper and should be an area for future research.

8 Conclusion

Methods have been developed to accurately compare the overall effect of the axial buckling load to different imperfection types. The results indicate that thickness imperfections hold the most influence over the axial buckling load than others and must be accounted for in the design process. Many more stochastic and probabilistic data are necessary to validate this approach. Such results may be used to aid the design of more robust, lightweight and cost-effective shells if used in collaboration with the Robust Index Methodology developed in previous work [9, 21].

References

[1] D. Bushnell. “Buckling of shells – pitfall for designers”. AIAA Journal, Vol. 19, No. 9, September, 1981.

[2] NASA. “Buckling of thin-walled circular cylinders”. NASA SP–8007, 1968.

[3] M. Hilburger, M. Nemeth, J. Starnes Jr. “Shell buckling design criteria based on manufacturing imperfection signatures”. AIAA J., Vol. 44, No. 3, pp 654–663, 2006.

[4] A. Takano. "Statistical knockdown factors of buckling anisotropic cylinders under axial compression". *Journal of Applied Mechanics* Vol. 79, 051004, pp 1-17, 2012.

[5] R. Degenhardt, A. Kling, A. Bethge, J. Orf, L. Kärger, R. Zimmermann, K. Rohwer, A. Calvi. "Investigations on imperfection sensitivity and deduction of improved knockdown factors for unstiffened CFRP cylindrical shells". *Composite Structures* Vol. 92, No. 8, pp 1939-946, 2010.

[6] R. Degenhardt. "DESICOS". DESICOS. European Union 7th Framework, Web. 06 Dec. 2012. http://www.desicos.eu.

[7] R. Zimmermann. "Buckling research for imperfection tolerant fibre composite structures". *Proc. of Proceedings of Conference on Spacecraft Structures, Materials and Mechanical Testing*, Grand Hotel Hats Ter Duia, Noordwijk, The Netherlands. 1996.

[8] C. Hühne, R. Zimmerman, R. Rolfes, B. Geier. “Sensitivities to geometrical and loading imperfections on buckling of composite cylindrical shells”. Rep. Germany: German Aerospace Centre, Braunschweig, Institute of Structural Mechanics, 2002.

[9] M. Lee. “Stochastic analysis and robust design of stiffened composite structures”. Diss. The University of New South Wales, 2009. Sydney: UNSWorks, 2009.

[10] M. Broggi, G. Schuëller. “Accurate prediction of the statistical deviations of the buckling load of imperfect CFRP cylindrical shells”. In: IV European Conference on Computational Mechanics. Paris, France, EU, 2010.

[11] D. Shillinger, V. Papadopoulos. “Accurate estimation of evolutionary power spectra for strongly narrow-band random fields”. Computer Methods In Applied Mechanics And Engineering, Vol. 199, No. 17-20, pp 947-960, 2010.

[12] I.M. Chakravarti, R.G. Laha, J. Roy. Handbook of methods of applied statistics. John Wiley and Sons; Vol. 1, pp 392-4, 1967.

[13] M. Chryssanthopoulos, V. Giavotto and C. Poggi. “Characterization of manufacturing effects for buckling-sensitive composite cylinders”. *Composite Manufacturing*, Vol. 6, No. 2, pp 93-101, 1995.

[14] A. Legrende. “*Nouvelles méthodes pour la détermination des orbites des comètes - Sur la Méthode des moindres quarrés*”. 1805.

[15] J. Kepple, B.G. Prusty, G. Pearce, D. Kelly, R. Thomson. “A new multi-objective robust optimization methodology”. *Proc. Of 7th Australasian Congress on Applied Mechanics*, The University of Adelaide, Adelaide, Australia. ACAM 7, 2012. Print. ISBN 978-1-9221076-1-9.

[16] C. Spearman, C. The proof and measurement of association between two things. *The American Journal of Psychology,* Vol 15, No. 1, pp 72-101, 1904.

[17] M. Hilburger, J. Starnes Jr. “Effects of imperfections on the buckling response of compression-loaded composite shells”. *International Journal of Non-Linear Mechanics*, Vol. 37, No. 4-5, pp 623-643, 2002.

[18] W.T. Koiter, The stability of elastic equilibrium, Ph.D. thesis, TU-Delft; 1945.

[19] B. Budiansky, J. Hutchinson, “Dynamic buckling of imperfection sensitive structures”. H. Gortler (Ed.), *Proceedings of the 11th IUTAM Congress*, Springer, Berlin pp 636-651, 1964.

[20] J. Árbocz, C.D. Babcock, “The effect of general imperfections on the buckling of cylindrical shells”.

Journal of Applied Mechanics, Vol. 36, No. 1, Series E, pp 28-38, 1969.

[21] R. Degenhardt. "COCOMAT." *COCOMAT*. Web. 07 Dec. 2012. http://www.cocomat.de.